# Cooperativity and Switching within the Three-State Model of Muscle Regulation†

Robin Maytum,‡ Sherwin S. Lehrer,§ and Michael A. Geeves*,‡

*Max Planck Institut für Moleculare Physiologie, D-44139 Dortmund, Germany, and Muscle Research Group, Boston Biomedical Research Institute, Boston, Massachusetts 02114*

*Received July 7, 1998; Revised Manuscript Received November 9, 1998*

ABSTRACT: Thin filament regulation is mediated by the presence of tropomyosin (Tm) and troponin (Tn) on the actin filament. Binding of Tm alone induces two states, closed and open (with the equilibrium between them defined by $K_T$), which differ in their affinity for myosin subfragment 1 (S1). Cooperative switching between the states results in characteristic sigmoidal myosin S1 binding curves. In the presence of Tn and absence of $Ca^{2+}$, a third state, blocked, has previously been kinetically shown to be present, leading to the three state model of McKillop and Geeves [(1993) *Biophys. J. 65*, 693−701]. We have measured equilibrium binding of S1 to phalloidin-stabilized pyrene−actin filaments by monitoring the pyrene fluorescence at 50 nM, a concentration 10-fold lower than previously possible. In combination with kinetic studies, we show that the data can be fitted to a modified version of the three-state model with an additional term allowing for a varying apparent cooperative unit size ($n$). Our results show that the apparent cooperative unit size ($n$) is dependent upon both the presence of Tn and of $Ca^{2+}$. Also in the absence of $Ca^{2+}$, the occupancy of the blocked state (defined by $K_B$) is accompanied by a 2−3-fold reduction in $K_T$. These results are discussed in comparison to the Hill model [(1980) *Proc. Natl. Acad. Sci. U.S.A. 77*, 3186−3190] and a flexible model of thin filament regulation based upon that of Lehrer et al. [(1997) *Biochemistry 36*, 13449−13455].

The regulation of the interaction between actin (A) and myosin heads (M) in skeletal muscle is brought about by a $Ca^{2+}$-induced change in the state of the thin filament proteins tropomyosin (Tm)[1] and troponin (Tn) (for reviews, see refs *1* and *2*).

The thin filament is a repeating structure made up of units of actin$_7$·TmTn. Skeletal tropomyosin is a linear coiled coil structure approximately 400 Å long which interacts with seven actin subunits and the troponin regulatory complex. This structural repeat containing seven actins per unit was used by Hill et al. (*3*) as the cooperative unit size in their model of thin filament cooperativity. A modification of this model was subsequently proposed by Geeves and Halsall (*4*), taking into account that binding of S1 to actin involves at least two steps after the formation of the collision complex.

McKillop and Geeves (*5*) more recently proposed that the regulation of TmTn-containing thin filaments can be interpreted in terms of a rapid $Ca^{2+}$-dependent equilibrium between three states of the thin filament, blocked, closed, and open. A steric blocking model of thin filament regulation has been proposed (Figure 1) which shows the relationship between the three states of the thin filament and the two-step binding of S1 to actin (*6*−*8*).

It was shown that in equilibrium measurements of S1 binding to actin·TmTn in the presence of $Ca^{2+}$, the relationship between $K_T$ and $K_2$ determined the form of the sigmoid titration curve (*9*). The blocked state is not occupied in the presence of $Ca^{2+}$. The ratio of open/closed thin filament cooperative units depends on the fraction of actin sites occupied by S1 and is defined by

$$\text{open/closed} = K_T(1 + K_2)^m$$

where $m$ is the number of actin sites within the cooperative unit occupied by S1. $K_T$ has a value of 0.2 in the presence of $Ca^{2+}$ and a value of $<0.2$ in the absence of $Ca^{2+}$, and as it is a property of the thin filament is independent of any nucleotide bound to the S1. In contrast, $K_2$ is a property of the S1 head and is independent of $Ca^{2+}$ binding to Tn.

In the absence of nucleotide, $K_2 \approx 200$, and a single S1 binding to a cooperative unit is sufficient to switch on the unit [i.e., $K_T(1 + K_2) \approx 40$]. The binding of different nucleotides to S1 allows $K_2$ to be varied from 0.3 to 200. As $K_2$ is reduced, the energy of binding of a single S1 becomes insufficient to turn on the cooperative unit. Therefore, several heads are required for activation, and this changes the form of the binding isotherm (*9*).

According to this model, binding profiles of S1 to actin have a sigmoidicity dependent upon the equilibrium ($K_T$) between the closed and open states and the size of the cooperative unit ($n$). Sigmoidicity was clearly demonstrated for titrations in both the presence of ADP, where $K_2 \approx 20$, and nucleotide analogues, where $K_2 < 20$. The sigmoidicity of these binding curves is also dependent upon the overall affinity for actin ($K_1K_2$), and since in the absence of

† Supported by NIH Grants HL 22461 and AR 41637.

* To whom correspondence should be addressed. Telephone: +49 231 1206 367. Fax: +49 231 1206 229. E-mail: geeves@mpi-dortmund.mpg.de.

‡ Max Planck Institut für Moleculare Physiologie.

§ Boston Biomedical Research Institute.

[1] Abbreviations: Tm, tropomyosin; Tn, troponin; S1, myosin subfragment 1; pyr-actin, pyrene-labeled actin; *n*, apparent cooperative unit size.

10.1021/bi981603e CCC: $18.00 
Published on Web 12/30/1998

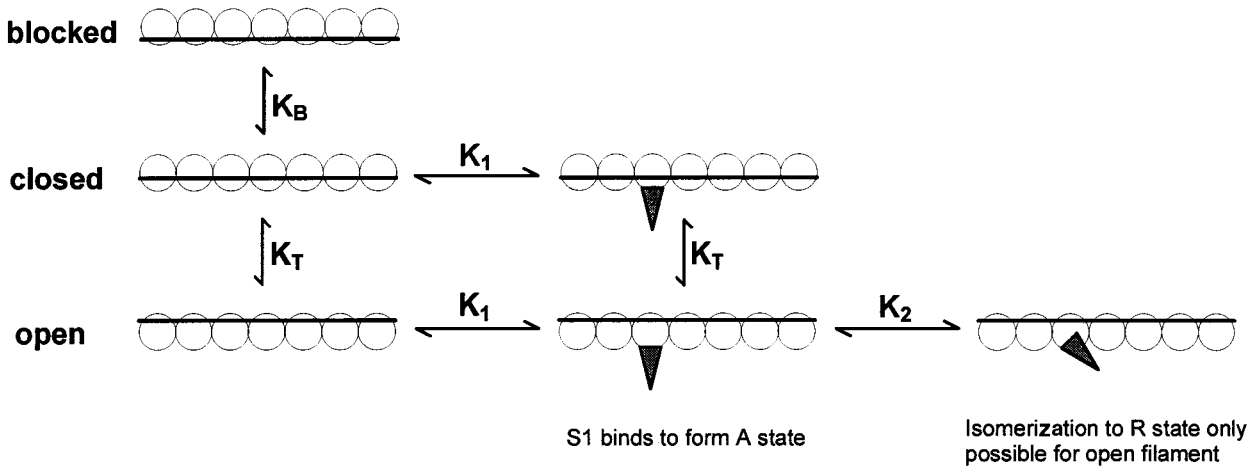


FIGURE 1: Three-state model of the thin filament as proposed by McKillop and Geeves (*9*). The $A_7$·TmTn structural unit is shown as seven open circles representing the actins connected via a line representing the tropomyosin. This unit exists in a dynamic equilibrium between the three states as represented by the different positions of tropomyosin. The three states are the blocked state in which no S1 binding can occur, the closed state in which only weak binding can occur, and the open state which allows isomerization of the S1 to the rigor-like state. The ratio of the three states in the absence of S1 is defined by the equilibrium constants $K_B$ (between the blocked and closed states) and $K_T$ (between the closed and open states). The blocked state is only present in the absence of $Ca^{2+}$ when the Tn complex is tightly bound to the filament; in the presence of $Ca^{2+}$, there is little or no occupancy of the blocked state, meaning $K_B$ is large and can be ignored.

nucleotide $K_2 \approx 200$, the apparent sigmoidicity at conventionally used actin and S1 concentrations is greatly reduced. A lower sigmoidicity results in less accurate determination of the binding parameters. To produce a significantly sigmoidal curve, the concentration of actin used should be in the same range as the overall affinity. However, the concentration that can be used is limited by two factors, the sensitivity of the assay system in measuring a change on binding and the equilibrium between filamentous and monomeric actin. If the concentration of actin is below the critical concentration, the actin will depolymerize, rendering the assay system useless. This limited the actin concentration which could be used in the equilibrium binding studies of McKillop and Geeves (*9*), and the fits were therefore not very sensitive to the size of the cooperative unit which was therefore assumed to be the $actin_7$·TmTn structural unit ($n = 7$).

Lehrer and Geeves (*10*) estimated the apparent cooperative unit size ($n$) using the excimer fluorescence of a pyrene label covalently attached to Cys-190 of Tm (Tm*) which reports the switch from the closed to open form of the filament. Comparison of light scattering (LS), which reports S1 binding to actin and the Tm* fluorescence (F), indicated the number of S1 molecules that must bind to or dissociate from an actin filament before it changes state in both equilibrium and kinetic measurements. For actin·Tm filaments, this was shown to be 1 in 6 actin sites occupied ($n = 6$) and 1 in 12 ($n = 12$) for an actin·TmTn filament; i.e., in the presence of troponin, the apparent cooperative unit is significantly greater than the $actin_7$·TmTn structural unit. The observation that $n$ under some conditions could be significantly greater than 7 (the size of the structural unit) led us to re-examine the binding data of McKillop and Geeves (*9*) and refine their method to allow more accurate determination of the binding curves.

It has recently been shown by Kurzawa and Geeves (*11*) that the large fluorescence change of pyrene-labeled actin stabilized with phalloidin can be used to measure myosin S1 affinity for actin at actin concentrations of <20 nM, allowing accurate determination of the S1 affinity in a stopped-flow assay. Using these principles, a titration system has been developed allowing S1 binding to be monitored in a continuous titration at similar low (50 nM) pyrene−actin concentrations under conditions where kinetic and mixing effects are negligible.

Using this technique, accurate curves for S1 binding to actin have been obtained in the presence of tropomyosin (Tm) and the complete regulatory complex (TmTn) under a variety of conditions. The binding curves can be fitted to a model based on that of McKillop and Geeves (*9*) including a varying cooperative unit size which has allowed determination of both the open/closed equilibrium ($K_T$) of the filament and the apparent cooperative unit size ($n$). The results show that $n$ is a property of the actin·Tm filament and dependent upon the presence of Tn and $Ca^{2+}$, but independent of ADP binding to S1. Furthermore, we confirm that $K_T$ in the presence of Tn is also $Ca^{2+}$-dependent.

However, the requirement for $n$ to vary dependent upon the titration conditions brings into question the definition of the cooperative unit size in terms of the structural unit. We consider the physical meaning of the apparent cooperative unit size and compare the analysis of this model with that of the earlier model of Hill et al. and the recent proposal that Tm should be considered a continuous flexible filament on the surface of actin (*20*).

## MATERIALS AND METHODS

*Proteins and Reagents*. Myosin subfragment 1 (S1) was prepared by chymotryptic digestion of rabbit myosin, as described by Weeds and Taylor (*12*). Its molar concentration was calculated from absorbance measurements at 280 nm using an $E^{1\%}$ of 7.9 $cm^{-1}$ and a molecular mass of 115 000 Da. Rabbit actin was purified by the method of Spudich and Watt (*13*). Its molar concentration was determined with its absorbance at 280 nm using an $E^{1\%}$ of 11.08 $cm^{-1}$ and a molecular mass of 40 000 Da. The preparation of pyrene-

labeled actin (pyr-actin) was like that previously described (*14*). Phalloidin-stabilized F-actin was made by incubating a solution of 10 $\mu$M pyr-actin with 10 $\mu$M phalloidin overnight in experimental buffer [20 mM MOPS (pH 7.0), 200 mM KCl, and 5 mM $MgCl_2$] at 4 °C.

*Stopped-Flow Experiments and Fluorescence Spectroscopy*. Stopped-flow experiments were performed at 20 °C with a Hi-Tech Scientific SF-61DX spectrophotometer in fluorescence mode. Pyrene fluorescence was excited at 365 nm and emission detected at right angles using a KV 389 nm cutoff filter (Schott, Mainz, Germany). Data were stored and analyzed using the Kinetasyst software provided with the instrument. Transients shown are the average of three to five shots of the machine. In these experiments, the concentrations quoted are those after mixing and are half the relevant concentrations of the stock solutions in the syringes.

Fluorescence titrations were performed on a SLM 8100 spectrofluorimeter at 20 °C using excitation at 365 nm with an 8 nm bandwidth and measuring emission at 405 nm with a 16 nm bandwidth. A total working volume of 2 mL was used in a 10 mm × 10 mm cell constantly being stirred with a magnetic stirrer below the light path of the instrument. Autotitrations were carried out using a Harvard Apparatus Syringe Infusion Pump 22 driving a 100 $\mu$L glass syringe (Hamilton). Injection was made through a port in the lid of the instrument directly into the cuvette below the surface of the solution, but above the light path. Data acquisition was triggered using a contact switch attached to the syringe/driveplate and connected to the TTL trigger input of the spectrofluorimeter. Data were acquired over a period of 250 s, with data points being collected every 0.5 s with an integration time of 0.45 s. Buffer solutions for the titrations were filtered using a 0.22 $\mu$m disposable syringe filter to remove dust particles which can produce significant noise in the stirred cell at the low levels of sample fluorescence used. Titration data are recorded with a continuous addition of a concentrated S1 stock solution using a syringe pump into a continuously stirred cell. The use of a 10 mm × 10 mm cell (2 mL volume) reduces the effects of dilution, as only 50 $\mu$L is added during a titration, and of fluorescence bleaching, as only a portion of the continuously mixed solution is exposed to the light path. The efficiency of mixing in the cell was checked by showing that addition of an unreactive fluorophor produced a linear change in fluorescence with no lag. The titration of actin with S1 was shown to be effectively in equilibrium by showing that halving the time scale of addition had no effect and that pausing a titration produced no further significant change in the fluorescence level as would be expected if the system were in equilibrium.

## MODELING

The equilibrium binding of S1 to unregulated actin conforms to a simple binding model.

$$A + M \overset{K_d}{\longleftrightarrow} A{\cdot}M$$

It can therefore be shown that a curve for titration of S1 against actin can be fitted to the following physically significant root of the quadratic equation.

$$\alpha = \frac{([M] + K_d + [A]_0) - \sqrt{([M] + K_d + [A]_0)^2 - 4/[M][A]_0}}{2[A]_0} \quad (1)$$

where $\alpha$ is the fraction of actin with S1 bound, [M] the total concentration of S1, $[A]_0$ the initial actin concentration, and $K_d$ the dissociation constant.

Binding can be monitored by the quenching of a pyrene label attached to actin. The fraction of actin bound is then directly proportional to the change in fluorescence.

$$\alpha = \frac{F_0 - F}{F_0 - F_\infty} \quad (2)$$

Generalizing the McKillop and Geeves (*9*) equation for the three-state model for a cooperative unit size *n* gives

$$\alpha = \frac{K_1[M]P^{n-1}\{K_T(1 + K_2)^n + 1\}}{(K_T P^n + Q^n + 1/K_B)(1 + K_2)^{n-1}} \quad (3)$$

where $\alpha$ is as defined in eq 2, [M] is the concentration of free S1, $P = 1 + K_1[M](1 + K_2)$, and $Q = 1 + K_1[M]$. As for the unregulated system, $\alpha$ can be related to the fractional change in pyrene fluorescence.

## RESULTS

To obtain precise S1−actin binding parameters by curve fitting the titration data, the concentration of actin used should be of the same order of magnitude (or lower) than the value of the overall binding constant ($K_1K_2$). In the case of titrations in the presence of TmTn, this means working at a concentration of ca. 50 nM. In previous studies (*9*, *15*), much higher actin concentrations have been used because of the necessity of keeping the actin in the filamentous (F) form or the relative insensitivity of the light scattering signal used to monitor binding. Kurzawa and Geeves (*11*) showed that phalloidin could be used to stabilize pyrene-labeled actin in the F form at low concentrations (1 nM) with little effect on the affinity of S1 for actin as monitored by fluorescence quenching of the pyrene label using stopped-flow techniques. A titration of pyr-actin (in the absence of TmTn) with S1 is shown in Figure 2. A fit to the data using eq 1, shown superimposed, gave a $K_d$ of 94 nM with $F_0$ and $F_\infty$ values of 42 000 and 19 090, respectively, i.e., an apparent quenching of around 55%. Using these low concentrations of pyr-actin, there is an appreciable level of background fluorescence or scatter from the solution. Hence, the level of fluorescence quenching is lower than the 70% expected for S1 binding to pyr-actin (*14*). The higher background also results in some variation in the $F_0$ values for titrations, although this is generally less than 5%. The value of $K_d$ determined using this method agrees with the value previously reported by Kurzawa and Geeves (*16*) under similar conditions.

The curve for a second titration in the presence of tropomyosin is sigmoid as expected for a cooperative binding curve. A large excess of tropomyosin was added (2 $\mu$M) over the 1:7 ratio theoretically required (7 nM) to ensure that the actin filaments were fully saturated with Tm as under these conditions the $K_d$ of tropomyosin for actin is ≈0.5 $\mu$M (*16*).

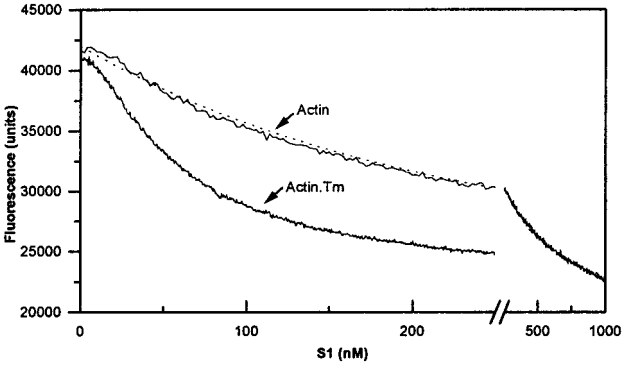


FIGURE 2: Titration of pyr-actin·phalloidin with myosin S1. S1 was added continuously to a stirred cuvette containing 50 nM pyr-actin·phalloidin. Binding is monitored by fluorescence quenching of the pyrene label upon S1 binding. The buffer was 20 mM MOPS, 200 mM KCl, and 5 mM $MgCl_2$ at 20 °C. Superimposed is a curve fit to the data using the quadratic solution of the equation of a simple binding model. $F_0$ and $F_\infty$ values were determined to be 42 000 and 19 090 for actin and 41 200 and 21 900 for actin·Tm, respectively.

Table 1: Parameters for Curve Fits in Figures 2 and 3

| | actin | Tm | Tm·Tn (with $Ca^{2+}$) | Tm·Tn (without $Ca^{2+}$) |
|---|---|---|---|---|
| $K_1$ ($\times 10^{-5}$ $M^{-1}$) | 0.532 | 1.33 | 0.98 | 1.22 |
| $K_2$ | 200 | 200 | 200 | 200 |
| $K_T$ | n/a | 0.155 | 0.143 | 0.033 |
| $n$ | n/a | 8 | 11 | 6 |
| $K_B$ | – | – | – | 0.5 |

Comparison of the midpoints of the titration curves shows that as well as inducing cooperativity, the presence of tropomyosin also results in a substantial increase in the affinity of S1 for actin. This has been previously shown to be an effect upon $k_{-1}$ as the rate constants of S1 binding to actin $k_{+1}$ and $K_2$ are unchanged (*4*).

The best fit using eq 3 is shown superimposed on the data, and the fitted parameters are listed in Table 1. Fitting data using eq 3 required an approach in which some of the parameters are defined and systematically varied, as a unique fit cannot be resolved when all parameters are allowed to vary simultaneously. As reported by McKillop and Geeves (*9*), the overall affinity is well-defined by the product $K_1K_2$, but the individual values of $K_1$ and $K_2$ are not separately defined. The value of $K_2$ is therefore fixed at the independently measured value of 200 (*5*). The blocked state is unoccupied ($K_B > 10$) and excluded from the fitting. The values of $n$ and $K_T$ are highly interdependent, but can be determined by systematic fitting. The value of $n$ was varied in integer values between 5 and 11, and the best fit to the curves based on the sum of squares, the standard deviations of the individually fitted parameters, and the residual plot gave a value of 8. The best fit values of $K_1$ and $K_T$ were $1.33 \times 10^5$ $M^{-1}$ and 0.155 with a standard deviation of 1 and 5%, respectively (Table 1). These are in good agreement with those previously obtained (*9*) and define the actin·Tm filament as being around 80% in the closed state in the absence of S1.

Figure 3A shows two titrations for actin·TmTn filaments in the absence and presence of $Ca^{2+}$. The data here and in subsequent plots are shown as the fraction of actin sites unoccupied by S1 for ease of comparison. Both curves show

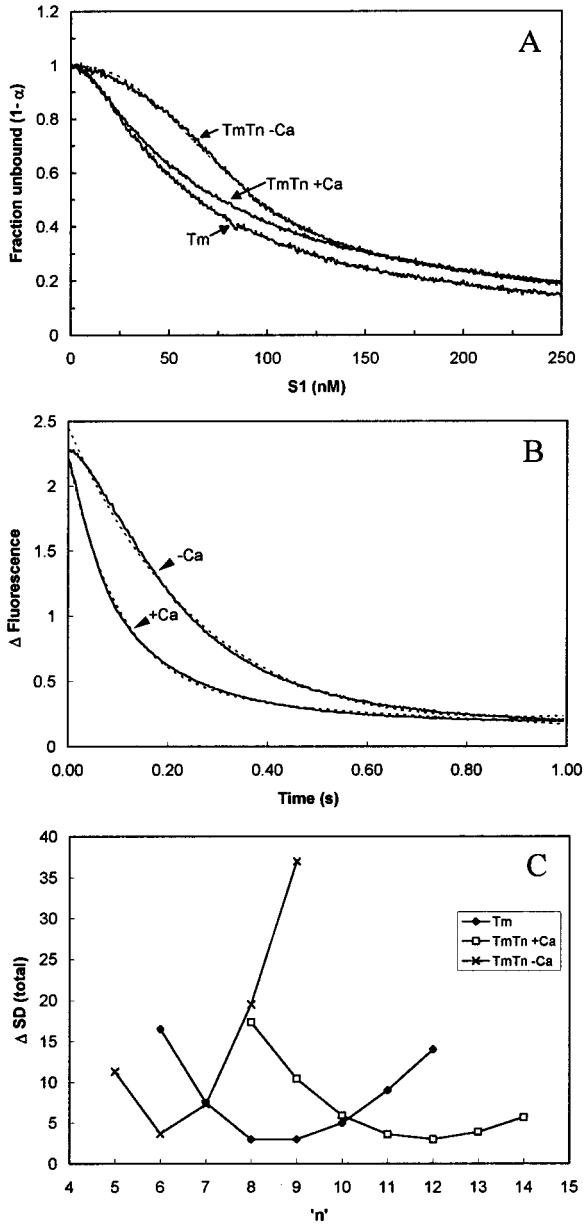


FIGURE 3: (A) Titrations of pyr-actin·phalloidin with S1 in the presence of either Tm (2 $\mu$M) or TmTn (0.1 $\mu$M). Conditions were like those described in the legend of Figure 2, except for the addition of either 1 mM $CaCl_2$ or 2 mM EGTA to the titrations in the presence of Tn. Superimposed on the data are curve fits using the binding model discussed in the text with the fitted parameters shown in Table 1. (B) Determination of the blocked state ($K_B$). Occupancy of the blocked state was determined by measuring the reduction in the rate of S1 binding to excess pyr-actin in the absence of $Ca^{2+}$. Shown are fluorescence quenching transient curves measured upon rapid mixing of 5 $\mu$M pyr-actin and 2 $\mu$M TmTn with 0.5 $\mu$M S1. Best fits to single exponentials are shown superimposed. Panel C shows the variation of the standard deviation of the fits as $n$ is varied for the data sets shown in panel A.

a sigmoid character which is much more pronounced in the absence of $Ca^{2+}$. The removal of $Ca^{2+}$ results in the occupancy of the blocked state, and $K_B$ must be independently determined for fitting with the other parameters. The value of $K_B$ was evaluated using the kinetic method established by McKillop and Geeves (*9*). The fluorescence changes observed on mixing an excess of pyr-actin·TmTn (5 $\mu$M) with 0.5 $\mu$M S1 in the presence and absence of $Ca^{2+}$ are shown in Figure 3B. Both curves are well described by

a single exponential but with the value of $k_{obs}$ in the absence of $Ca^{2+}$ being approximately $^1/_3$ of that in the presence of $Ca^{2+}$. The value of $K_B$ is defined by

$$\frac{k_{obs+Ca}}{k_{obs-Ca}} = 1 - \frac{1}{1 + K_B(1 + K_T)} \text{ and hence } K_B \approx 0.5$$

The data in Figure 3A were fitted using the same procedure that was used for the data for Tm alone, using the calculated value for $K_B$ for the fit to the data in the absence of $Ca^{2+}$. The best fits are shown superimposed, with the fitted values listed in Table 1. As outlined earlier, the fits were repeated for integer values of *n*, and the values of the fitted parameters for the best fit are reported in the tables. In Figure 3C, we show the variation in the total standard deviation [$\sqrt{\Sigma}$(fit-data point)$^2$] for the data shown in Figure 3A. The minimum standard deviation can be readily identified, with the value of *n* defined to within $\pm 1$ for actin·Tm and actin·TmTn with $Ca^{2+}$. For these data sets, *n* is relatively independent of the other parameters. For actin·TmTn in the absence of $Ca^{2+}$, *n* is better defined but the fitted values of *n* and $K_B$ are not independent. The value of *n* is sensitive to $K_B$ where $K_B \approx 1$; at large and small values of $K_B$, *n* approaches 7. $K_B$ and $K_T$ are also interdependent, and the data can be fitted equally well with a $K_B$ of $\gg 10$ (i.e., no blocked state) with a much smaller value of $K_T$. The value of *n* derived is therefore dependent upon the value of $K_B$ obtained in the independent kinetic measurement, but its value will not be outside the range of 5−7. With these provisions, all of the parameters of eq 3 are well defined by the titration curves and the data establish two novel results; the value of $K_T$ is $Ca^{2+}$ sensitive, and the value of *n* depends on both the presence of Tn and $Ca^{2+}$ binding to Tn.

The value of $K_1$ does not change significantly between the titrations and is a little smaller than the value for titration of Tm alone. $K_T$ for TmTn in the presence of $Ca^{2+}$ (0.14) is similar to that for Tm alone (0.16), with a significantly smaller value in the absence of $Ca^{2+}$ (0.03). In the presence of $Ca^{2+}$, $n \approx 11$, which, as expected from the data of Lehrer and Geeves (*10*), is larger than in the presence of Tm alone ($n \approx 8$). More surprisingly, the value of *n* is reduced to 6 when $Ca^{2+}$ is removed.

The results of these titrations and analyses therefore extend the work of McKillop and Geeves (*9*) and confirm that the value of $K_T$ is $Ca^{2+}$ sensitive, changing from 0.15 to 0.05 on removal of $Ca^{2+}$. In addition, the value of *n* is dependent upon both the presence of Tn and that of $Ca^{2+}$. These conclusions were further tested by varying the titration conditions and evaluating the effect upon the fitted values of $K_T$ and *n*. If these conclusions are correct, then the binding of ADP to S1 should only affect those parameters concerned with S1 binding ($K_1$ and $K_2$) and have no effect on $K_T$, $K_B$, or *n* as these are properties of the actin filament in the absence of S1. This approach has been used previously by Greene et al. (*17*) and subsequently by McKillop and Geeves (*5*) to evaluate titration data.

Titrations in the presence of 2 mM ADP for S1 versus pyr-actin·Tm or pyr-actin·TmTn in the presence and absence of $Ca^{2+}$ are shown in Figure 4. The data show essentially the same features as in the absence of ADP except the overall affinities were reduced by a factor of around 40 as expected (*9*, *15*). The data were evaluated as before using a value for

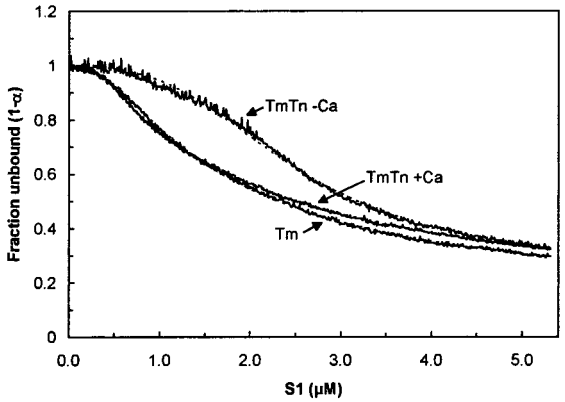


FIGURE 4: Titrations of 50 nM pyr-actin·phalloidin with S1 in the presence of either Tm (2 $\mu$M) or TmTn (0.1 $\mu$M). Conditions were like those described in the legend of Figure 2, except for the addition of 2 mM ADP, 50 $\mu$M $Ap_5A$, 2 mM glucose, and 2.5 units of hexokinase to all titrations. Superimposed are curve fits to the data using the binding model discussed in the text, the parameters for which are listed in Table 2.

Table 2: Parameters for Curve Fits in Figure 4

| | Tm | Tm·Tn (with $Ca^{2+}$) | Tm·Tn (without $Ca^{2+}$) |
|---|---|---|---|
| $K_1$ ($\times 10^{-4}$ $M^{-1}$) | 2.08 | 1.91 | 2.44 |
| $K_2$ | 20 | 20 | 20 |
| $K_T$ | 0.152 | 0.138 | 0.057 |
| *n* | 8 | 12 | 6 |
| $K_B$ | − | − | 0.5 |

$K_2$ of 20 (*5*) and for $K_B$ of 0.5 in the absence of $Ca^{2+}$. The same pattern seen before can be seen in the fitted parameters shown in Table 2. $K_1$ is almost invariant for the three titrations and is 5-fold smaller than in the absence of ADP. Values for $K_T$ and *n* are similar to the values in the absence of ADP for the three titrations; i.e., $K_T$ is unchanged on addition of Tn to the actin·Tm filament in the presence of $Ca^{2+}$ and is reduced if $Ca^{2+}$ is removed. The value of *n* increases from around 8 for actin·Tm to 11−12 on binding Tn and is reduced to 6−7 in the absence of $Ca^{2+}$. Thus, the two sets of titrations are in agreement.

As a second test of the model and fitting procedure, the titrations for TmTn were repeated at low ionic strengths. McKillop and Geeves (*9*) and Head et al. (*18*) evaluated the value of $K_B$ as a function of ionic strength and showed that at KCl concentrations below 50 mM the value of $K_B$ became large, consistent with the loss of the blocked state. However, the ATPase of S1 in the presence of actin·TmTn remained $Ca^{2+}$ sensitive, being one reason for the conclusion that $K_T$ was $Ca^{2+}$ sensitive. More recent studies in this laboratory have shown that the loss of the blocked state at low ionic strengths was due to the low magnesium concentration used (2 mM; Ritchie, unpublished observation). The TmTn titrations were therefore repeated at 30 mM KCl in the presence of 2 mM ADP and either 5 or 2 mM $MgCl_2$. The proportion of blocked state was evaluated in each case from the rate of S1 binding to an excess of pyr-actin·TmTn as shown in panels B and D of Figure 5. The $k_{obs}$ values in the presence and absence of $Ca^{2+}$ were 19 and 9 $s^{-1}$ for 5 mM $MgCl_2$ and 24 and 27 $s^{-1}$ at 2 mM $MgCl_2$, respectively. This yields values for $K_B$ of $\geq 10$ at 5 mM and 0.75 at 2 mM $MgCl_2$, respectively.

Table 3: Parameters for Curve Fitting to the Hill Model

| | Tm | Tm·Tn (with $Ca^{2+}$) | Tm·Tn (without $Ca^{2+}$) |
|---|---|---|---|
| K1 ($\times 10^{-4}$ $M^{-1}$) | 2.0 | 2.0 | 2.0 |
| K2 ($\times 10^{-5}$ $M^{-1}$) | 4.54 | 3.97 | 3.72 |
| $L'$ | 5.75 | 3.66 | 33.6 |
| $Y$ | 1.52 | 4.46 | 1.64 |

Table 4: Parameters for Curve Fits in Panels A and C of Figure 5

| | Tm·Tn and 5 mM $MgCl_2$ | | Tm·Tn and 2 mM $MgCl_2$ | |
|---|---|---|---|---|
| | with $Ca^{2+}$ | without $Ca^{2+}$ | with $Ca^{2+}$ | without $Ca^{2+}$ |
| $K_1$ ($\times 10^{-5}$ $M^{-1}$) | 7.72 | 8.57 | 12.0 | 10.7 |
| $K_2$ | 20 | 20 | 20 | 20 |
| $K_T$ | 0.216 | 0.045 | 0.204 | 0.061 |
| $n$ | 11 | 8 | 11 | 8 |
| $K_B$ | – | 0.75 | – | – |

The fluorescence titrations of S1·ADP in the presence and absence of $Ca^{2+}$ are shown for the two $Mg^{2+}$ concentrations in panels A and C of Figure 5 with best fits overlaid upon the data. These show the expected sigmoidal curves, which were fitted as for previous data with $K_2$ set at 20 in all cases and $K_B$ at 0.75 for the without $Ca^{2+}$ data set at 5 mM $MgCl_2$. For the 2 mM $MgCl_2$ without $Ca^{2+}$ data set, $K_B$ was deemed to be large and excluded from the fitting process. The matching data set in the presence of $Ca^{2+}$ is not sufficiently sigmoidal to give a defined fit if all parameters are allowed to float, even using the same fitting approach as outlined previously. However, if $K_1$ is fixed to a value similar to that derived from the without $Ca^{2+}$ data (as would be expected from all previous results), a good fit can be produced with values in good agreement with the other fits. The values derived from the fits are shown in Table 4 for the 5 and 2 mM data sets. It can be seen that $K_1$ is significantly higher for the 2 mM $MgCl_2$ data sets ($\approx 8 \times 10^5$ $M^{-1}$) in comparison to the 5 mM $MgCl_2$ data sets ($\approx 12 \times 10^5$ $M^{-1}$) due to the difference in ionic strength between the buffers caused by the differing contributions of $MgCl_2$ in either case. However, it can be seen that despite the apparent loss of the blocked state at 2 mM $MgCl_2$, the fitted values for $K_T$ ($\approx$0.2 and $\approx$0.04) and $n$ (11 and 8) are similar at high and low $MgCl_2$ concentrations. Thus, the values of $K_T$ and $n$ are relatively independent of $MgCl_2$ concentration, ionic strength, and the presence of ADP.

## DISCUSSION

This work represents an appreciable improvement in the accuracy of the determination of the binding parameters for binding of S1 to regulated actin. These improvements allowed the titrations to be accomplished at concentrations that were $^1/_{10}$ of the previously used actin concentrations, giving greater accuracy to the fitted parameters. In earlier work (*4*, *9*), the titrations were insensitive to the apparent cooperative unit size ($n$), and this was fixed at the size of the structural unit ($n = 7$). We now show that the value of $n$ can be extracted from the titration data and that the values of both $n$ and $K_T$ depend on the presence of Tn and $Ca^{2+}$.

*$Ca^{2+}$ Dependence of $K_T$.* The data presented confirm that the value of $K_T$ is $Ca^{2+}$-dependent as suggested by McKillop and Geeves, although they were unable to explicitly determine the values. Measurement of $K_T$ in the presence and absence of ADP showed that in both cases the value changed

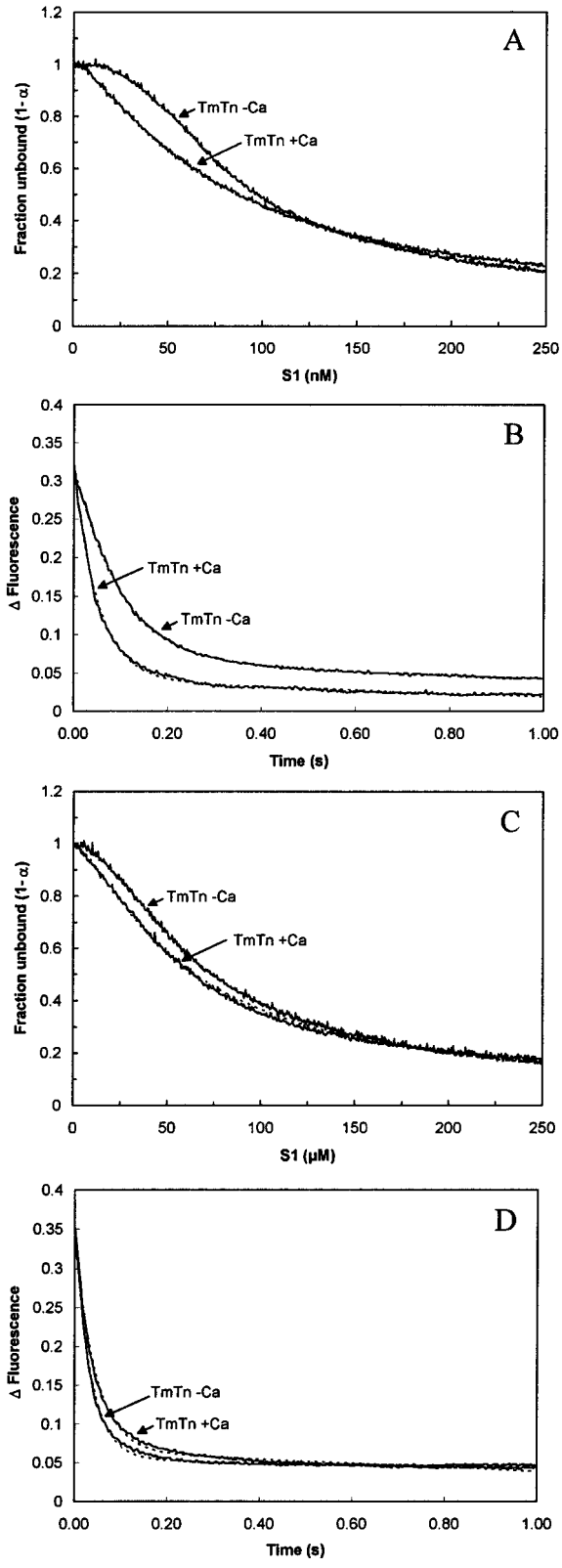


FIGURE 5: (A and C) Titrations of pyr-actin·phalloidin (50 nM) with TmTn (0.1 $\mu$M) with S1 in the presence (1 mM $CaCl_2$) and absence (2 mM EGTA) of $Ca^{2+}$. The buffer was 20 mM MOPS and 30 mM KCl and either (A and B) 5 mM $MgCl_2$ or (C and D) 2 mM $MgCl_2$. Superimposed are curve fits to eq 3, the parameters for which are listed in Table 4. (B and D) Determinations of the blocked state for the titrations. Pyr-actin (5 $\mu$M) and 2 $\mu$M TmTn were mixed with 0.5 $\mu$M S1 under the same buffer conditions described for the respective titrations. Binding rates (19 and 9 $s^{-1}$ and 24 and 29 $s^{-1}$ with or without $Ca^{2+}$, respectively) were determined by single-exponential curve fits which are shown superimposed on the data.

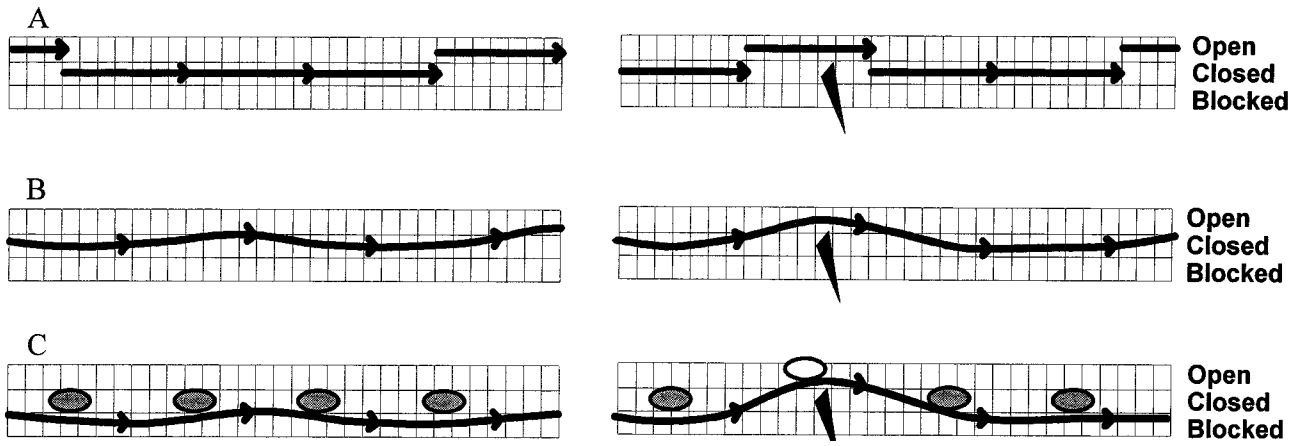


FIGURE 6: Schematic diagram of the thin filament showing the traditional rigid tropomyosin model and a flexible tropomyosin model. Actin subunits are shown diagramatically as having three sites, representing the blocked, open, and closed states of the three-state model. The left side shows a section of thin filament in the absence of S1, and the right side shows the effect of the binding of a single S1 head in the rigor state. In panels A and B, the filament is shown in the presence of $Ca^{2+}$ and Tn or when Tn is absent. In these cases, the Tm exists in an equilibrium between the closed and open states. (A) Tm is shown as described by Hill et al. as a rigid rod spanning seven actin monomers moving as a single unit between the two positions, the filament being open 20% of the time. The presence of a rigor-like S1 traps the adjacent Tm in the open state. The presence of Tn and $Ca^{2+}$ increases the likelihood of adjacent Tms changing state at the same time. (B) Tm is shown as a continuous dynamically disordered flexible rod again occupying the same proportion of the open state. The extent of cooperativity is defined by the stiffness and persistence length of the continuous Tm filament, the presence of Tn (particularly the TnT component) increasing the stiffness and persistence length. (C) The thin filament in the presence of Tn and absence of $Ca^{2+}$. The strongly bound inhibitory TnI domains (gray ovals) every seven actins constrain the Tm to the blocked and closed states. The 30% occupancy of the closed state experimentally observed may represent the flexibility of the Tm between TnI sites or the binding equilibrium between TnI and actin. Binding of S1 necessitates the release of the immediately juxtaposed TnI domain (shown unshaded), but the two adjacent TnI domains remain strongly bound, thus reducing the number of additional actins turned on by a single S1. For the rigid Tm model, this would have the effect of reducing the interaction between adjacent Tms.

from 0.15 to 0.05 on removal of $Ca^{2+}$. To examine whether this change was an artifact due to larger changes in $K_B$, the measurements were repeated under conditions where there appears to be little occupancy of the blocked state. The data presented establish that it is the combination of low ionic strength and low $Mg^{2+}$ concentration (<3 mM) which causes the loss of the blocked state. At 5 mM $Mg^{2+}$ (where the blocked state is appreciably occupied, $K_B = 0.75$ in the absence of $Ca^{2+}$ ) and 2 mM $Mg^{2+}$ (little or no occupancy of the blocked state, $K_B \gg 1$), the values of $K_T$ (0.2 and 0.06 in the presence and absence of $Ca^{2+}$, respectively) are only a little larger than those under high-salt conditions. The value of $K_T$ at 2 mM $Mg^{2+}$ with no $Ca^{2+}$ is a little higher than at 5 mM. This supports the conclusion that the closed to open transition is $Ca^{2+}$ sensitive.

*$Ca^{2+}$ and Troponin Dependence of n*. Our fits to the data show that *n* has a value of approximately 7 for an actin·Tm filament similar to the size of the structural unit, and this increases to 11 for an actin·TmTn filament in the presence of $Ca^{2+}$. These values of *n* are in good agreement with those measured using a different method of Lehrer and Geeves (*10*) for the case of actin·Tm and actin·TmTn with $Ca^{2+}$. The interpretation favored by them was that the presence of TnT in the Tm−Tm overlap region increased the level of Tm−Tm communication, leading to an increase in the size of the apparent cooperative unit. This conclusion is supported by the increased value of *n* measured in the presence of the Tn fragment $TnT_1$ (*19*) and the larger value of *n* measured for actin·Tm filaments in which the Tm's have stronger end to end interactions such as smooth muscle Tm and fibroblast Tm 5a (*21*).

Removal of $Ca^{2+}$ reduces *n* to a value close to that seen in the absence of Tn. This reduction in *n* observed in the absence of $Ca^{2+}$ may be the result of the troponin complex pinning the Tm down every 7 actins, therefore reducing the level of information transfer between adjacent TmTn complexes (see Figure 6). However, *n* remains small at low salt and low $Mg^{2+}$ concentrations in the absence of $Ca^{2+}$, where there is no blocked state, suggesting that there is still a $Ca^{2+}$ sensitive troponin effect as shown by the change in $K_T$.

The value of *n* for actin·TmTn filaments did not decrease in the absence of $Ca^{2+}$ when measured using the kinetic method of Lehrer and Geeves (*10*). In this experiment, they measured the rate of dissociation of S1 by ATP from a fully decorated actin·TmTn filament (light scattering signal) and estimated how many S1 molecules must dissociate before the Tm returned to the closed state (excimer fluorescence of Tm*). Thus, the measurement is of the rate of formation of the closed state from an open state and not the blocked to open transition as measured here. As discussed later, the two transitions represent two different structural changes in the filament, and the cooperativity of the open to closed and blocked to closed transitions need not be the same. We will also consider below the physical meaning of *n*.

*Comparison to the Hill Model*. An earlier version of a cooperative binding model for S1 and actin·TmTn was proposed by Hill et al. (*3*). This is closely related to the model of Geeves and Halsall (*4*) in that the $actin_7$·TmTn units can exist in two states (on and off) with the equilibrium position defined by $L'$ (off/on) equivalent to $1/K_T$ from the model of Geeves and Halsall. The affinity of S1 for the two states is defined by the two association constants K1 and K2, respectively, which are identical to $K_1$ and $K_1(1 + K_2)$ in the model of Geeves and Halsall. In addition, the Hill model allowed for additional cooperativity between adjacent actin·TmTn units. This was described by a nearest neighbor model where the interaction between units is stronger when they are in the same state, the parameter *Y* defining the extent of

this additional cooperativity. In the work of Geeves and Halsall (*4*) and McKillop and Geeves (*9*), no evidence of cooperativity was observed beyond that within the actin$_7$·TmTn unit, so no additional cooperativity factor was included in their analysis. As pointed out by Hill et al. in their original work (*3*), the inclusion of additional cooperativity by an increase in the apparent cooperative unit size is roughly equivalent to the modeling of nearest neighbor interactions using the factor *Y*. This is illustrated in Table 3 which shows the parameters determined by fitting the data of Figure 4 to the equations of Hill et al. (*3*). As can be seen, the values of K1 and $K_1$ ($2.0 \times 10^4$ $M^{-1}$), K2 and $K_1(1 + K_2)$ ($4 \times 10^5$ $M^{-1}$) are equivalent under all conditions as are the values of $1/L'$ and $K_T$ for actin·Tm (0.15 and 0.17, respectively) and actin·TmTn in the presence of $Ca^{2+}$ (0.14 and 0.27, respectively). However, in the absence of $Ca^{2+}$, $1/L'$ is equivalent to $K_B(1 + 1/K_T)$ as the equations of Hill et al. have no equivalent of the blocked state. The value of *Y* of 1.5 is compatible with little Tm−Tm cooperativity as shown from the alternative fits which give a value of *n* approximately equal to 7. As seen with the fits using our model, only the TmTn filament in the presence of $Ca^{2+}$ shows a larger value of *Y* (4.5) which is compatible with the larger value of *n* (11−12) determined here. The data of Greene (*21*) showed that for a range of different nucleotides (none, ADP, or AMP-PNP) the ratio of K1 to K2 was sensitive to the nucleotide bound to S1 (in agreement with the model of Halsall and Geeves where $K_2$ is nucleotide-dependent), and the values of $L'$ and *Y* (which are properties of the thin filament) did not vary with the nucleotide in agreement with this work. However, the data were not sensitive to changes in the value of *Y* in the presence of $Ca^{2+}$ due to the limited resolution of the data and reduced sigmoidicity of the binding curves at the high actin concentrations used (1.3−50 $\mu$M). Further studies by Williams and Greene (*22*) were unable to distinguish between binding curves for Tm and TmTn in the presence of $Ca^{2+}$ for the same reasons despite evidence for differences from ATPase measurements (*23*, *24*). The work of Ishii and Lehrer (*10*) in which they used pyrene-labeled Tm to measure switching of the actin$_7$·TmTn units from closed to open states allowed greater sensitivity, and fits by them using the Hill model showed that TmTn in the presence of $Ca^{2+}$ had a larger value of *Y* than in the absence of $Ca^{2+}$ or absence of Tn. This is in agreement with the data presented here, although the value of *Y* in the absence of $Ca^{2+}$ was higher than that determined by us (5 vs 1.6). Thus, both models are capable of representing the observed behavior of regulated thin filaments, and we can therefore ask which model gives a better description of the switching of the filament.

We have shown that in terms of fitting the titration data both our model and that of Hill et al. will produce good fits. It must be appreciated however that the equilibrium data only describe the formation of the open state of the filament from blocked and closed states, which is why for our model the data for the blocked state must be determined separately by kinetic methods. The Hill model which contains no blocked state is only capable of representing the equilibrium data as its two states are incompatible with the kinetic data.

Both the models of Hill et al. and Geeves and Halsall and McKillop and Geeves are based upon the structural unit of actin$_7$·TmTn with a rigid Tm switching a cooperative unit of seven actin subunits as shown in Figure 6A. The position of S1 binding within the structural unit has no influence on its ability to switch the unit and adjacent units (Hill et al.) between states. The data presented here show that additional cooperativity is required to describe the system, and this is possible in the Hill model but not in the model of McKillop and Geeves. However, as shown here, the model of McKillop and Geeves can describe the cooperativity using an apparent cooperative unit size (*n*) of >7. While the term *Y* is functionally equivalent to *n*, it should be noted that both parameters relate to what are mathematically discontinuous Tm models; i.e., the Tm filament consists of a series of separate units which switch between discrete states.

The rigid model of Tm has dominated much of the thinking about Tm models since the original formulation of the steric blocking model. Structural data from both electron microscopy (*25*) and X-ray diffraction studies (*26*) suggest that Tm makes quite large movements over the actin surface between the three states. In a rigid model, this would require large changes in the Tm−Tm contacts to allow a single Tm to change state. Yet Tm−Tm contacts are very important for the binding of Tm to actin (*27*−*29*) and in some views provide the majority of the binding energy for the formation of the actin·Tm filament. This is supported by the observation that Tm lacking the N-terminal acetylation shows an at least 1 order of magnitude reduction in affinity for actin (*30*). In these respects, models representing Tm as rigid sections which are not necessarily continuous with their neighbors cannot be favored. The work of Lehrer et al. (*20*) with pyr·Tms showed that the apparent cooperativity was not dependent upon the length of Tm but upon Tm−Tm interactions. This led to the proposal of Tm existing as a flexible filament which has an apparent cooperative unit size *n* based upon the filament properties and not the size of the structural unit. The flexible model shown in panels B and C of Figure 6 illustrates the essential features of the Tm filament on the actin surface. Tm is represented as a continuous dynamic thread along the actin surface which in the absence of Tn (or with Tn and $Ca^{2+}$) spends 80% of its time in the closed position and 20% in the open position. The binding of a single S1 into the R state traps the Tm at that actin site in the open state. The number of adjacent actins with Tm in the open state is then a function of the dynamic flexibility of the Tm around the fixed point defined by S1. The stiffer the Tm filament, the further the information about the S1 binding is transmitted. For an TmTn filament in the absence of $Ca^{2+}$, the strong actin−TnI interaction provides an additional anchor between Tm and actin every seven actin sites and thus reduces the persistence length of any changes in Tm position on the actin surface. The modified model of McKillop and Geeves used here does not describe the continuous Tm model accurately except at low levels of S1 saturation. Under these conditions, the switched units are centered without overlap around S1 binding sites, and the parameter *n* describes the average number of adjacent actins switched as governed by the Tm filament flexibility. In this respect, *n* can be considered an indicator of cooperativity in much the same way as the classically defined Hill coefficient (A. Hill, 1913) is used for globular cooperative enzymes.

The flexible model described here provides a qualitative explanation for the large values of *n* measured and for the changes in *n* observed on addition of Tn and removal of

$Ca^{2+}$. However, the model as described by eq 3 is at best an approximation of the actin filament at low levels of saturation with myosin. The challenge is now to define the persistence length and flexibility model in mathematical terms that can be applied to all conditions and to test this model using both structural and dynamic measurements coupled with the use of recombinant Tms of varying length and flexibility.

## ACKNOWLEDGMENT

We thank Nancy Adamek for her excellent technical assistance and the support of Prof. Roger Goody of the Max-Planck Institut für Molekulare Physiologie.

## REFERENCES

1. Lehrer, S. S. (1994) *J. Muscle Res. Cell Motil. 15*, 232−236.
2. Lehrer, S. S., and Geeves, M. A. (1998) *J. Mol. Biol. 277*, 1081−1089.
3. Hill, T. L., Eisenberg, E., and Greene, L. (1980) *Proc. Natl. Acad. Sci. U.S.A. 77*, 3186−3190.
4. Geeves, M. A., and Halsall, D. J. (1987) *Biophys. J. 52*, 215−220.
5. 5. McKillop, D. F. A., and Geeves, M. A. (1991) *Biochem. J. 279*, 711−718.
6. Geeves, M. A., Goody, R. S., and Gutfreund, H. (1984) *J. Muscle Res. Cell Motil. 5*, 351−361.
7. Geeves, M. A. (1991) *Biochem. J. 274*, 1−14.
8. Geeves, M. A., and Connibear (1995) *Biophys. J. 68* (Suppl. 4), 194S−199S.
9. McKillop, D. F. A., and Geeves, M. A. (1993) *Biophys. J. 65*, 693−701.
10. Lehrer, S. S., and Geeves, M. A. (1994) *Biophys. J. 67*, 273−282.
11. Kurzawa, S. E., and Geeves, M. A. (1996) *J. Muscle Res. Cell Motil. 17*, 1−8.
12. Weeds, A. G., and Taylor, R. S. (1975) *Nature 257*, 54−57.
13. Spudich, J., and Watt, S. (1971) *J. Biol. Chem. 246*, 4866−4871.
14. Criddle, A. H., Geeves, M. A., and Jeffries, T. E. (1985) *Biochem. J. 232*, 343−349.
15. Ishii, Y., and Lehrer, S. S. (1990) *Biochemistry 29*, 1160.
16. Wegner, A. (1979) *J. Mol. Biol. 108*, 839−853.
17. Greene, L., and Eisenberg, E. (1980) *Proc. Natl. Acad. Sci. U.S.A. 77*, 2616−2620.
18. Head, J. G., Ritche, M. D., and Geeves, M. A. (1995) *Eur. J. Biochem. 227*, 694−699.
19. Schaertl, S., Lehrer, S. S., and Geeves, M. A. (1995) *Biochemistry 34*, 15890−15894.
20. Lehrer, S. S., Golitsina, N. L., and Geeves, M. A. (1997) *Biochemistry 36*, 13449−13455.
21. Greene, L. (1982) *J. Biol. Chem. 257*, 13993−13999.
22. Williams, D. L., and Greene, L. E. (1983) *Biochemistry 22*, 2770−2774.
23. Lehrer, S. S., and Morris, E. P. (1982) *J. Biol. Chem. 257*, 8073−8080.
24. Nagashima, H., and Asakura, S. (1982) *J. Mol. Biol. 155*, 409−428.
25. Vibert, P., Craig, R., and Lehman, W. (1997) *J. Mol. Biol. 266*, 8−14.
26. Homes, K. C. (1995) *Biophys. J. 68*, 2s−5s.
27. McLallan, A. D., and Stewart, M. (1976) *J. Mol. Biol. 103*, 271−298.
28. Phillips, G. N., Jr., Fillers, J. P., and Cohen, C. (1986) *J. Mol. Biol. 192*, 111−131.
29. Cho, Y.-J., Liu, J., and Hitchcock DeGregori, S. E. (1990) *J. Biol. Chem. 265*, 538−545.
30. Heald, R. W., and Hitchcock DeGregori, S. E. (1988) *J. Biol. Chem. 263*, 5254−5259.

BI981603E